SCIENTIFIC REPORTS

OPEN

SUBJECT AREAS:
OCEANOGRAPHY
ADAPTATION
CLIMATE CHANGE
BIODIVERSITY

Received
14 May 2012

Accepted
11 June 2012

Published
5 July 2012

The submarine volcano eruption at the island of El Hierro: physical-chemical perturbation and biological response

E. Fraile-Nuez[1¥], M. González-Dávila[2*], J. M. Santana-Casiano[2*], J. Arístegui[2*], I. J. Alonso-González[3†], S. Hernández-León[2*], M. J. Blanco[4], A. Rodríguez-Santana[5], A. Hernández-Guerra[2*], M. D. Gelado-Caballero[5], F. Eugenio[2*], J. Marcello[2*], D. de Armas[1], J. F. Domínguez-Yanes[1¥], M. F. Montero[2*], D. R. Laetsch[3†], P. Vélez-Belchí[1¥], A. Ramos[6‡], A. V. Ariza[2*], I. Comas-Rodríguez[2*] & V. M. Benítez-Barrios[1¥]

[1]Instituto Español de Oceanografía, Centro Oceanográfico de Canarias (IEO-COC). Santa Cruz de Tenerife, Spain, [2]Universidad de Las Palmas de Gran Canaria, Instituto de Oceanografía y Cambio Global (IOCAG). Las Palmas, Spain, [3]Universidad de Las Palmas de Gran Canaria, Banco Español de Algas (BEA). Las Palmas, Spain, [4]Instituto Geográfico Nacional, Centro Geofísico de Canarias. Santa Cruz de Tenerife, Spain, [5]Universidad de Las Palmas de Gran Canaria, Facultad de Ciencias del Mar. Las Palmas, Spain, [6]Universidad de Las Palmas de Gran Canaria, Instituto Universitario de Sistemas Inteligentes y Aplicaciones Numéricas en Ingeniería (IUSIANI). Las Palmas, Spain

Correspondence and requests for materials should be addressed to E.F.-N. (eugenio.fraile@oceanografia.esca.ieo.es)

*Instituto de Oceanografía y Cambio Global (IOCAG).

† Banco Español de Algas (BEA).

‡ Instituto Universitario de Sistemas Inteligentes y Aplicaciones Numéricas en Ingeniería (IUSIANI).

¥ Área de medio marino y protección ambiental (IEO-COC).

On October 10 2011 an underwater eruption gave rise to a novel shallow submarine volcano south of the island of El Hierro, Canary Islands, Spain. During the eruption large quantities of mantle-derived gases, solutes and heat were released into the surrounding waters. In order to monitor the impact of the eruption on the marine ecosystem, periodic multidisciplinary cruises were carried out. Here, we present an initial report of the extreme physical-chemical perturbations caused by this event, comprising thermal changes, water acidification, deoxygenation and metal-enrichment, which resulted in significant alterations to the activity and composition of local plankton communities. Our findings highlight the potential role of this eruptive process as a natural ecosystem-scale experiment for the study of extreme effects of global change stressors on marine environments.

Active submarine volcanoes constitute a significant source of mantle-derived gases, solutes and heat to the ocean. Their emissions react with seawater leading to important physical-chemical anomalies that may strongly impact the marine ecosystem[1,2]. However, the impacts of short-term submarine volcanic activity on the surrounding biota, especially planktonic communities, are still poorly understood. Here, we provide evidence that one of the richest and most sensitive marine ecosystems of the subtropical northeast Atlantic Ocean has been dramatically affected by the recent submarine eruption at the island of El Hierro (Canary Islands).

Results

After three months of volcanic unrest, characterized by more than 10,000 earthquakes (M≤4.3) and 5 cm of ground deformation, on October 10 2011 the national seismic network recorded a substantial decrease of seismicity together with continuous volcanic tremor, indicating the beginning of an eruptive phase. Since then, regular multidisciplinary monitoring has been carried out in order to quantify environmental impacts caused by the submarine eruption (Figure 1).

Periodic bathymetric measurements located the main vent 1.8 km offshore of the southern coast of El Hierro and indicated a major uplift of the volcano, raising it from 300 m depth to just 88 m below the surface. Conductivity-Temperature-Depth measurements of the waters affected by the volcanic emissions revealed temperature and salinity anomalies of +3°C and −0.3, respectively, at 80 m depth and 290 m from the volcano. Maximum temperature anomalies of +18.8°C were observed over the crater at 210 m depth using expendable bathythermograph probes (Figure 2). The release of CO_2 produced total inorganic carbon concentrations ranging from 4,000 to 7,500 μmol kg^{-1} causing water acidification of up to 2.8 units within the first 100 m depth and 2 km from the volcano. These high CO_2 levels generated high pCO_2 (partial pressure of CO_2) waters with values ranging from 12,000 to 150,000 μatm at the surface. The most affected part of the water column was the layer

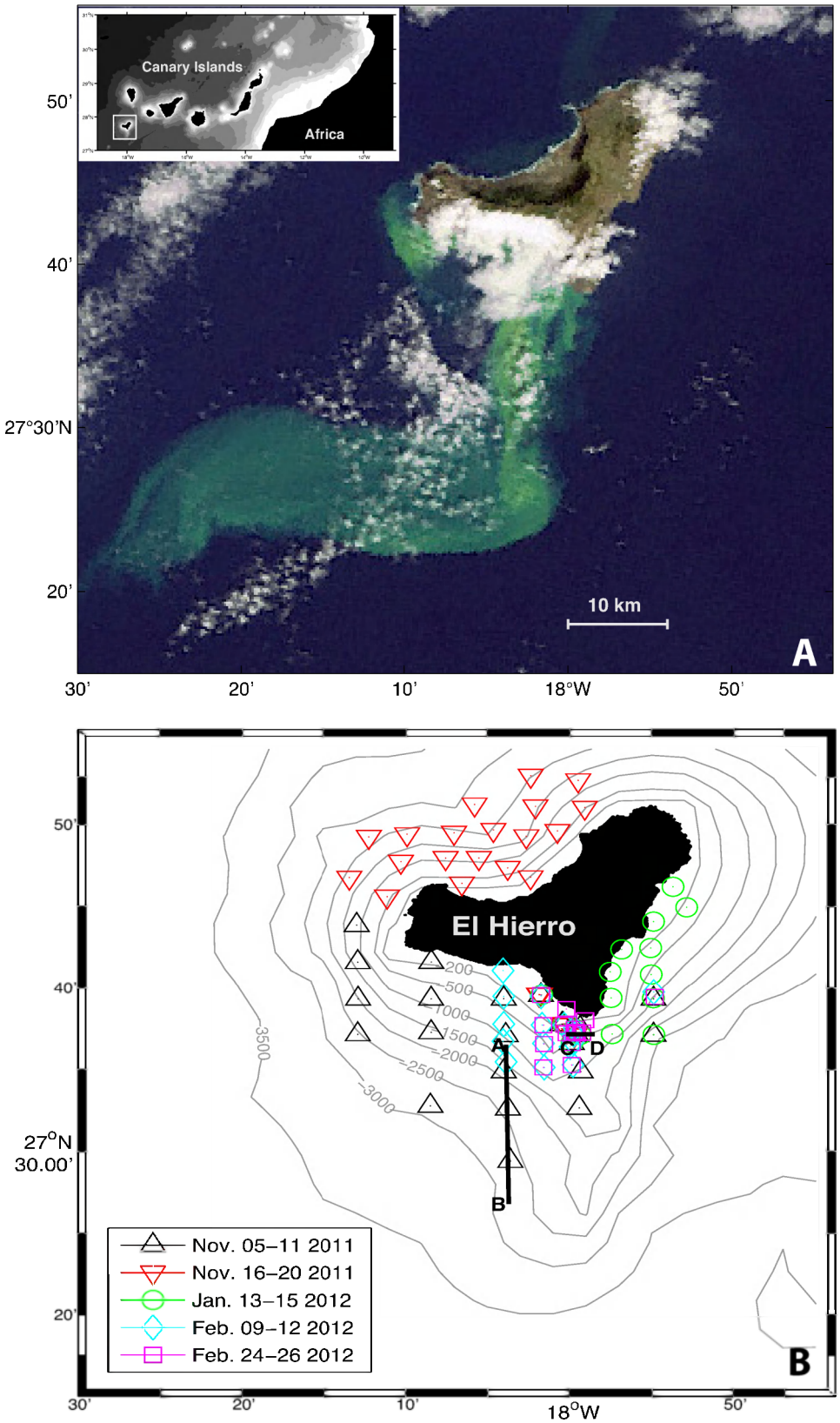

Figure 1 | (A) Natural color composite from the *MEdium Resolution Imaging Spectrometer (MERIS)* instrument aboard ENVISAT Satellite (European Space Agency), (November 9, 2011 at 14:45 UTC). Remote sensing data have been used to monitor the evolution of the volcanic emissions, playing a fundamental role during field cruises in guiding the Spanish government oceanographic vessel to the appropriate sampling areas. The inset map shows the position of Canary Islands west of Africa and the study area (solid white box). (B) Location of the stations carried out from November 2011 to February 2012 at El Hierro. Black lines denote transects A-B (Figure 3) and C-D (Figure 5).

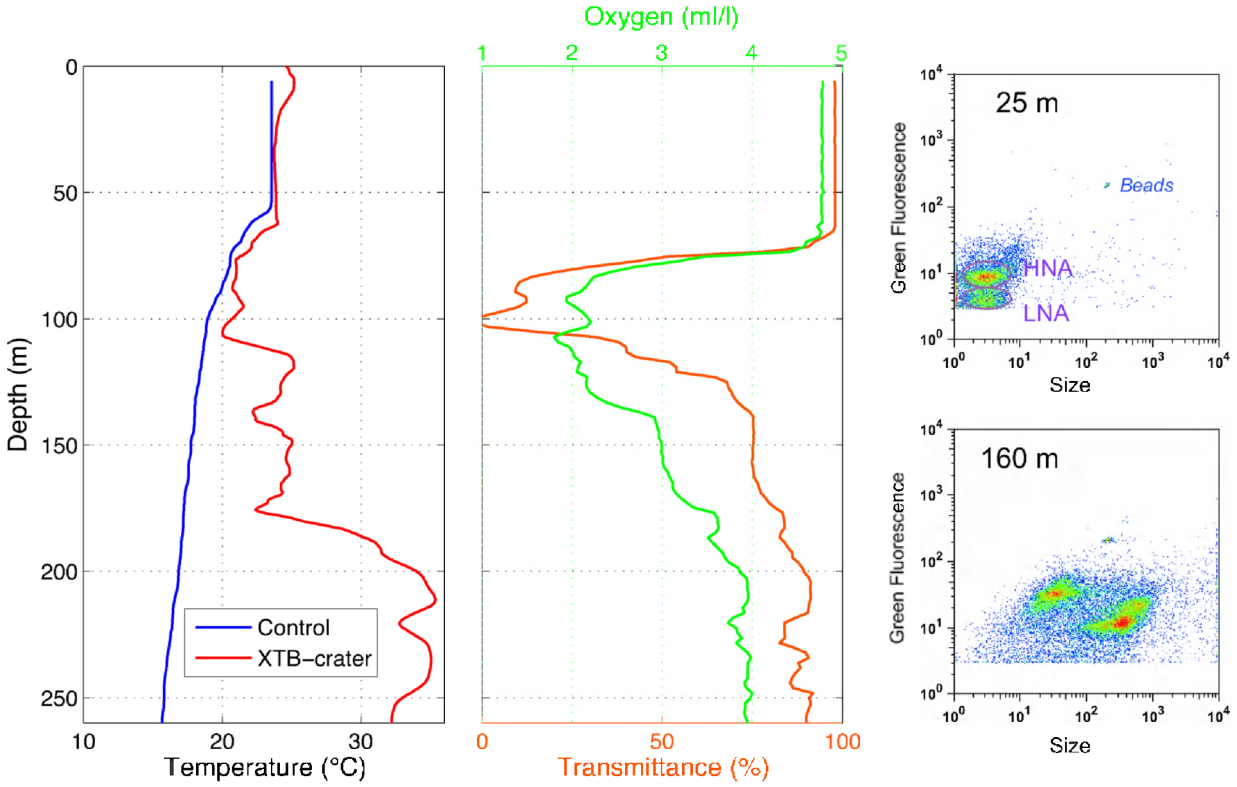

Figure 2 | Vertical profiles of temperature, dissolved oxygen and transmittance at the volcano station. Flow cytometry plots of green fluorescence versus side scatter (size) identify different bacterial groups at 25 m and 160 m. HNA and LNA (High/Low Nucleic Acid content bacteria) are typical bacteria groups found in the water column outside the area of volcanic influence.

from 75 to 125 m depth which experienced oxygen depletion near to anoxic levels, enhanced light attenuation (transmittance decrease), negative redox potential, pH decrease, maximum concentrations of reduced sulfur and total Fe(II) species (200 and 50 μmol kg^{-1}, respectively) and higher concentrations of dissolved Cu, Cd, Pb and Al with maximum values of 6.1, 6.7, 5.8 and 2,122 nM, respectively.

These physical-chemical anomalies had a major impact on local pelagic communities. No fish schools were acoustically detected within the volcano affected area, and many dead fish were observed floating at the surface. Due to low light penetration, the upper limit of the deep scattering layer (produced by plankton and nekton echoes) was around 100 m shallower than usual in waters affected by the volcano. There, diel vertical migration was rather weak or absent as a consequence of anoxic levels in shallow layers (Figure 3). Small picoplankton communities showed a variable response to the volcanic emissions. Picophytoplankton at surface layers were not affected. However, at 75 m depth, *Prochlorococcus* showed a three-fold and *Synechococcus* a two-fold significant decline of abundance (t-test, $p<0.06$ and $p=0.1$, respectively), compared to far-field stations. Conversely, heterotrophic bacterial abundances (particularly large cells with high green fluorescence) increased dramatically with depth at stations affected by the volcanic emissions. The distinct response of the picophytoplankton groups to the volcano's influence is suggestive of ecotype selection under the rapidly changing conditions. Indeed, preliminary phylogenetic analyses of 16S rDNA from surface waters revealed *Prochlorococcus* ecotypes characterized by lower chlorophyll b/a ratios and higher cupric ion tolerance (High Light-adapted[3], HLI and HLII) (Figure 4). The lack of HLI ecotypes in waters affected by the volcanic emissions may indicate a

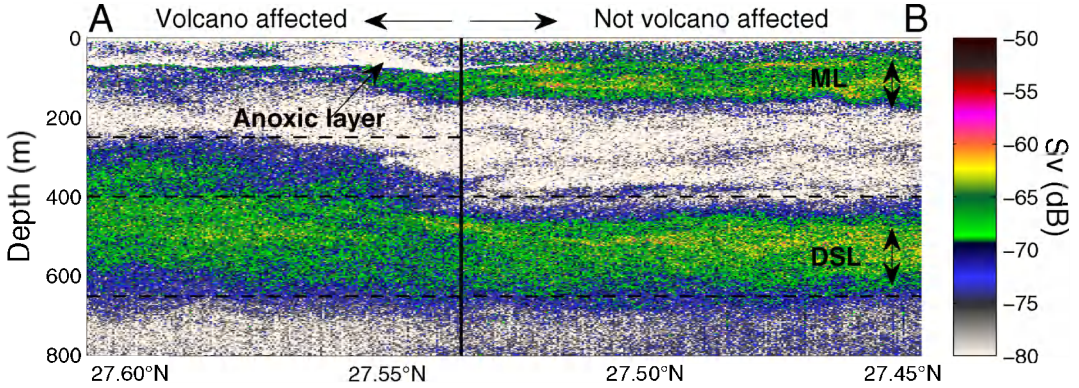

Figure 3 | Night echogram from a 38 kHz echo sounder showing vertical distribution of the migrant and Migrant and Deep Scattering Layers (ML and DSL) across the volcano affected area. Color bar refers to volume backscattering strength (S_v) in decibels.

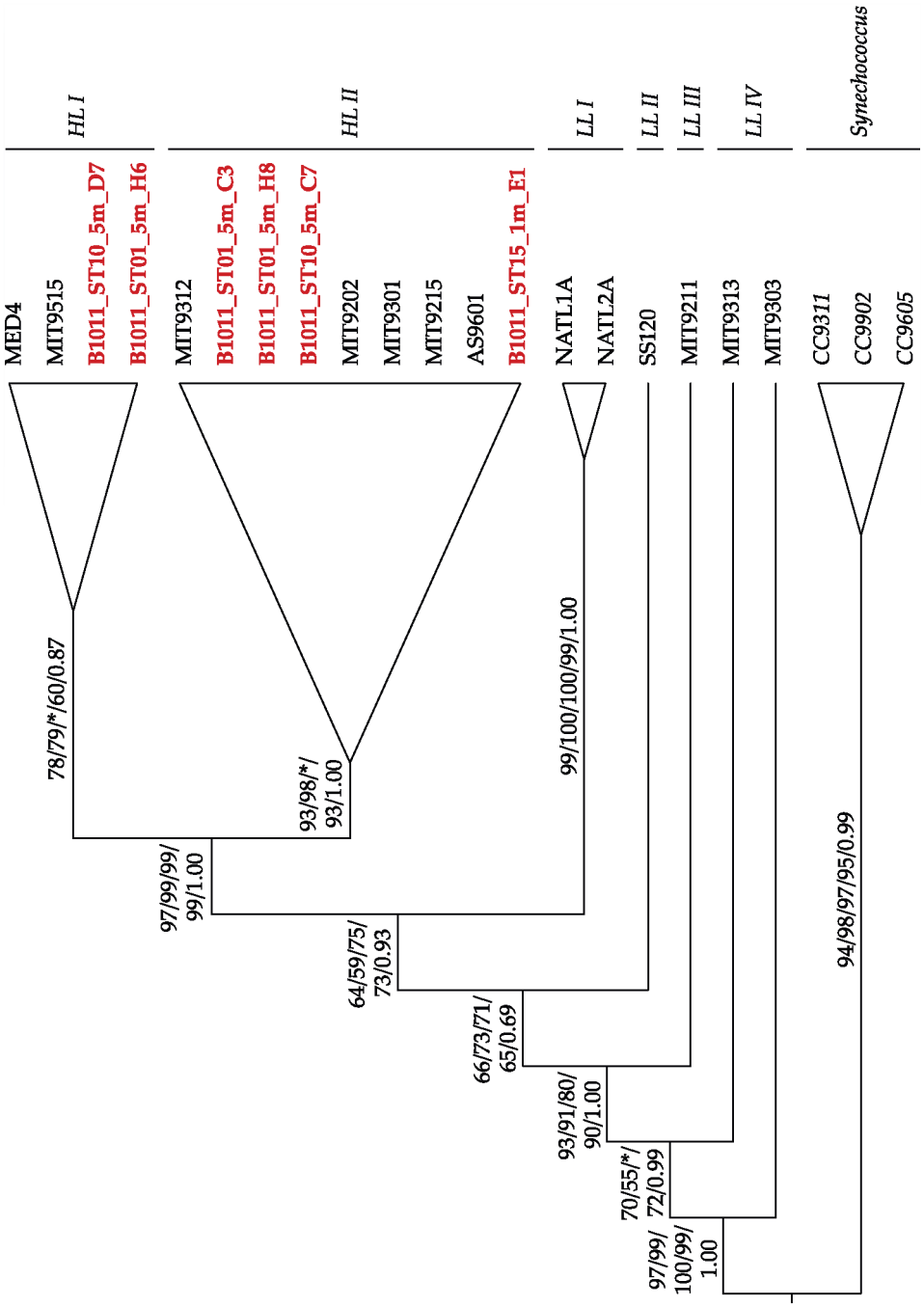

Figure 4 | Phylogenetic tree based on Neighbour-Joining (NJ), LogDet, Maximum Parsimony (MP), Maximum Likelihood (ML) and Bayesian inference (BI). *Synechococcus* strains were used as an out-group. Bootstrap supports and Bayesian posterior probabilities are indicated on each branch (NJ/LogDet/MP/ML/BI). * = Not present.

volcano-induced selection towards higher growth-temperature optima, an attribute associated with the HLII ecotypes.

Five months after the beginning of the eruptive process, monitoring of the physical-chemical properties around the volcano continues to show significant variations within the different fields being measured (Figure 5). Surface temperature and salinity above the crater show small but notable differences of +0.02°C and −0.018, respectively. Although CO_2 values have decreased considerably since the eruption, they continue to be highly variable. pCO2 ranges between 16,000 and 19,000 µatm (compared with 150,000 µatm at the time of the eruption), and surface pH values show a decrease of 1.8 points below normal levels to 6.2.

Discussion

During the eruption of a submarine volcano at the island of El Hierro, volcanic emissions resulted in major physical-chemical alteration of the surrounding waters, such as warming, acidification and deoxygenation. These three processes are also the main stressors of global climate change, driven primarily by elevated anthropogenic release of carbon dioxide into the atmosphere[4]. Global climate models predict for the next century a rise of 0.6°C in ocean surface temperature[5], a decrease of 0.3 – 0.4 pH units in surface waters[6], and a decline of 1 – 7% in the global ocean oxygen inventory[7]. Marine organisms have already responded to these changes through variations in their distribution and survival[8], decreased calcification

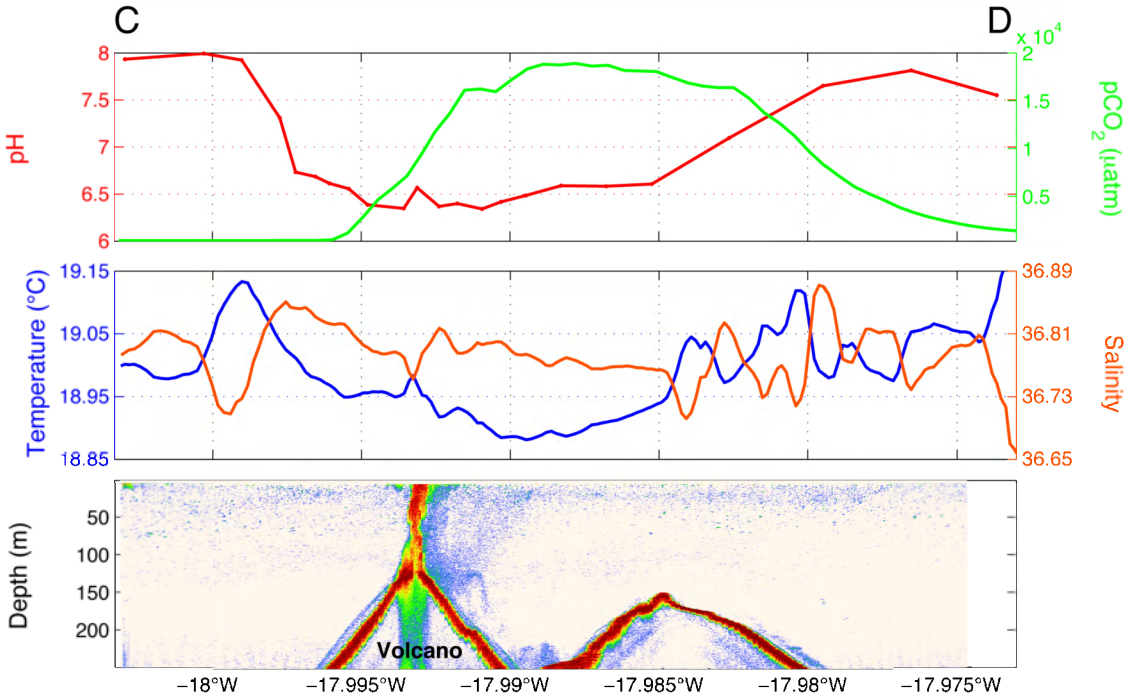

Figure 5 | Surface measurements of pH, pCO_2, temperature and salinity along a transect across the volcano still show significant variations five months after the beginning of the eruptive process. Bottom panel shows an echogram from a 70 kHz echo sounder.

rates[6] and alteration of diurnal and ontogenetic vertical migrations of pelagic communities[9,10]. These effects directly impact the structure and functioning of marine ecosystem.

The volcano affected area has exhibited responses that are occurring globally, making El Hierro into a unique natural laboratory where the principal climate change stressors are acting simultaneously. The results emerging from this volcanic eruption will help to improve our understanding of how future climate change may impact marine biota.

Methods

Hydrography. Vertical profiles of conductivity, temperature, pressure, oxygen and transmittance were collected using a SeaBird 9/11-plus CTD equipped with dual conductivity and temperature sensors. CTD sensors were calibrated at the SeaBird laboratory before the cruise. Water samples were obtained using a rosette of 24 10-liter Niskin bottles.

Acoustics. Vessel-mounted Simrad EK60 (38 and 70 kHz) split-beam echosounders were used to collect acoustic data. During the acoustic tracks, average navigation speed, temporal resolution (ping rate) and pulse length were 3 kn, 1 s^{-1} and 1.024 ms, respectively, for both frequencies. Acoustic raw data were post-processed with LSSS software.

$pH_{T,25}$. pH was measured on the total scale at a constant temperature of 25°C ($pH_{T,25}$) using two different techniques. The UV-Vis spectrophotometric technique[11] that used the m-cresol purple as an indicator[12] removes the dye effect for each pH reading. The standard deviation for the measurements was ± 0.002. The potentiometric technique was used in the stations that were more affected by the submarine volcanic emissions. A ROSS™ combined glass pH electrode was used. The electrode was calibrated using a Tris/HCl buffer in synthetic seawater[13]. The standard deviation for the potentiometric pH measurements was ± 0.005.

Total dissolved inorganic carbon and total alkalinity. The VINDTA 3C (Marianda, Germany) was used for the determination of both total dissolved inorganic carbon and total alkalinity. The VINDTA 3C was connected to a coulometer to determine the total dissolved inorganic carbon[14]. Total alkalinity was determined[15] on the VINDTA 3C using differential potentiometry. The certified reference material for oceanic CO_2, CRMs batch #105, was used to test the performance of both total inorganic carbon and total alkalinity, resulting in a precision of ±1.0 µmol kg^{-1} for both parameters.

pCO_2. pCO_2 was calculated from total dissolved inorganic carbon and pH data using the set of constants[16,17].

Fe(II). The concentration of Fe(II) was determined by UV-Vis spectrophotometry using a 5-m-long waveguide capillary flow cell (LWCFC) from World Precision Instruments. A modified version of the Ferrozine method was used[18,19]. The standard deviation of the method was ± 1 nM of Fe(II). Samples were diluted when necessary in order to achieve a nanomolar range of concentrations.

Reduced S species. The term reduced S species is defined as the sum of both hydrogen sulfide dissolved in water (H_2S) together with the products of its dissociation (HS^-, S^{2-}), and the reduced compounds of sulfur (colloid sulfur, S^0), sulfites (SO_3^{2-}), polysulfides (S_x^{2-}) and polythionates ($S_2O_3^{2-}$, $S_4O_6^{2-}$). These species were determined by the iodometric method[20,21] using an automatic potentiometry titrator equipped with a platinum electrode (Metrohm). The method presented a standard deviation of ± 1 µM kg_{sw}^{-1}.

Soluble Metals. Samples from the Niskin bottles were stored in 250 ml Nalgene bottles and immediately frozen (−20°C) until analysis at a land-based laboratory. To prevent contamination, all containers were previously cleaned using 3 M HNO_3 (1 week) and 0.1 M HCl (1 week), and rinsed thoroughly with ultra high purity water after each step. Samples were cleaned-filtered through 0.2 µm acid washed Nucleopore filter in a Class-100 laminar flow clean bench. Analysis of trace metal concentrations was carried out by High Speed Scan Cathodic Stripping Voltammetry (HSACSV) using a polarographic system[22] and a mercury drop electrode (EG&G, 303A) with a Ag-AgCl reference and platinum counter electrode. The standard addition method was used for quantifying trace metals in the samples. The procedure for the determination of dissolved aluminium[23] in seawater is based on the complexation of Al by 1,2-dihydroxyanthroquinone-3-sulphonic acid (DASA). Samples were prepared in Teflon cups of polarographic cells, containing 10 ml of water, $2 \cdot 10^{-6}$ M DASA and 0.01 M BES (7.1 pH). The DASA-Al peak appears at ca. −1.25 V. Oxygen was removed by purging the solution with nitrogen for 5 minutes. Metal analysis was performed in a diluted solution to avoid drop saturation. The voltammetric procedure for Cu, Pb and Cd was carried out in unpurged seawater using a background scan correction. pH was adjusted to 7.6 by addition of 100 µl of 1 M HEPES and 20 µl of $4 \cdot 10^{-3}$ M oxine (8-quinolinol). Copper, lead and cadmium peaks appear at −0.52 V, −0.62 V and −0.87 V, respectively.

Flow Cytometric analysis. Heterotrophic bacteria (HB), small photosynthetic eukaryotic cells (picoeukaryotes, PE), and *Prochlorococcus* (Pro) and *Synechococcus* (Syn) type cyanobacteria were counted by flow cytometry using a FACScalibur. To count HB, samples (4 ml) were fixed with 2% final concentration of paraformaldehyde, incubated for 15–30 min at 4°C and then stored frozen in liquid nitrogen until analyzed. Then, 200 µl were stained with a DMSO-diluted SYTO-13 (Molecular Probes Inc.) stock (10:1) at 2.5 µM final concentration. The identification of small phytoplankton groups (Pro, Syn and PE) was based on interactive analysis of multiple bivariate scatter plots of side scatter, red and orange fluorescence without staining. Samples were run at low speed for HB and at medium or high speed for phytoplankton until at least 10,000 events were acquired. A suspension of yellow–

green 1 μm latex beads (~10^5 beads ml^{-1} for phytoplankton and ~10^6 beads ml^{-1} for HB) was added as an internal standard (Polysciences, Inc.). Cell abundances were calculated from bead concentrations. The bead solution was checked daily by epifluorescence microscopy counting.

DNA extraction. Samples (50 ml) were filtered through 50 μm polycarbonate filters and 0.2 μm pore size cellulose acetate syringe filters. The cellulose acetate filters were stored in liquid nitrogen. For DNA extraction, the filter membranes were extracted using sterile scissors and forceps and processed using the NucleoSpin® Plant II kit (Macherey-Nagel, Germany) with a Proteinase K (Takara, Japan) digestion step (0.2 mg/ml) at 55°C for 1 h. DNA concentration and purity was determined by spectrophotometry and DNA was stored at −20°C.

rDNA clone libraries and sequencing. Partial rDNA operons (>4,400 nt from 16S rDNA-Helix 4 [H39] to 23S rDNA-Helix H4 [H2735]) were amplified using universal SSU rRNA (SSU-4-forw, 5′-GATCCTKGCTCAGGATKAACGCTGGC-3′) and cyanobacterial- specific ptLSU (CD-rev, 5′-GCCGGCTCATTCTTCAAC-3′)[24] primers. PCR reactions (25 μl) contained 75 ng DNA, primers (0.4 μM), dNTPs (200 μM), 1X KAPATaq buffer and 0.5 U/μl KAPATaq DNA polymerase (KAPA Biosystems, USA), and was subjected to the following program: 95°C for 3 min, 30 cycles of 95°C for 1 min, 55°C for 2 min and 72°C for 3 min, and 72°C for 5 min. Clone libraries were constructed using the TOPO TA Cloning® Kit (Invitrogen, USA) following manufacturer's instructions (pCR®2.1-TOPO® vector, TOP10 *Escherichia coli* cells). Positive clones were used as template for an additional PCR reaction. PCR products were purified using the NucleoSpin® Extract II kit (Macherey-Nagel GmbH & Co. KG, Germany) and sequencing was performed at a commercial sequencing service (Macrogen Inc., Korea) using the primers: Seq_16S_H4_forw (5′-TKGCTCAGGATKAACGCTGGC-3′), Seq_16S_pos874_forw (5′-ACTCAAAGGAATTGACG-3′), Seq_16S_39_rev (5′-ACTTAACCCRACATCTCACGACACG-3′) and Seq_16S_49_rev (5′-TACGGCTACCTTGTTACGACTTC-3′)[25].

Alignment and phylogenetic analyses. Six *Prochlorococcus* sequences were identified by BLAST[26] and deposited on GenBank [JQ670967-JQ670972]. These sequences were combined with 16S rDNA database sequences of *Prochlorococcus* strains (MED4: BX548174, MIT9515: CP000552, MIT9312: CP000111, MIT9202: AF115269, MIT9301: CP000576, MIT9215: CP000825, AS9601: CP000551, NATL1A: CP000553, NATL2A: CP000095, SS120: AE017126, MIT9211: CP000878, MIT9313: NC_005071, MIT9303: CP000554) and *Synechococcus* (outgroup) strains (CC9902: CP000097, CC9311: CP000435, CC9605: CP000110) and manually aligned using SEAVIEW4[27] considering the 16S rDNA secondary structure of *Synechococcus* sp. PCC6301. Alignments are available upon request. A total of 1,397 unambiguously aligned positions were used for analyses with maximum likelihood (ML), Bayesian inference (BI), distance methods (NJ), and maximum parsimony (MP). ML was performed using RAxML v7.2.8[28] for 10 runs and 1,000 (thorough) bootstrap (BS) replicates under the GTR+I+Γ model. BI was carried out through MrBayes v3.1.2[29] with two independent MCMC runs of four Metropolis-coupled chains under the GTR+I+Γ model, assuming default priors. Chains were sampled every 1.000 generations for 5x10^6 generations. Convergence of chains was assessed using Tracer 1.5 (http://tree.bio.ed.ac.uk/software/tracer/) and the first 500 trees were discarded as burn-in. NJ was carried out using SEAVIEW4[27] performing 1,000 BS replicates under the HKY model and using LogDet distances. MP was carried out using PHYLIP v3.52 (http://evolution.genetics.washington.edu/phylip.html) with 10 random starts, 1,000 BS replicates and retaining the best 10,000 trees.

1. Hall-Spencer, J. M. *et al.* Volcanic carbon dioxide vents show ecosystem effects of ocean acidification. *Nature* **454**, 96 (2008).
2. Resing, J. A. *et al.* Chemistry of hydrothermal plumes above submarine volcanoes of the Mariana. *Arc. Geochem. Geophys. Geosyst.* **10**, Q02009, doi:10.1029/2008GC002141. (2009).
3. Johnson, Z. I. *et al.* Niche partitioning among Prochlorococcus ecotypes along ocean-scale environmental gradients. *Science* **311**, 1737 (2006).
4. Gruber, N. Warming up, turning sour, losing breath: ocean biogeochemistry under global change. *Phil. Trans. R. Soc. A* **369**, 1980, doi:10.1098/rsta.2011.0003 (2011).
5. Intergovernmental Panel on Climate Change. Summary for Policymakers. In Climate Change 2007: The Physical Science Basis. Working Group I Contribution to the Fourth Assessment Report of the IPCC (eds Solomon, S. *et al*), Cambridge Univ. Press, Cambridge (2007).
6. Orr, J. C. *et al.* Anthropogenic ocean acidification over the twenty-first century and its impact on calcifying organisms. *Nature* **437**, 681–686 (2005).
7. Keeling, R. F., Körtzinger, A. & Gruber, N. Ocean deoxygenation in a warming world. *Annu. Rev. Mar. Sci.* **2**, 199–229 (2010).
8. Burrows, M. T. *et al.* The pace of shifting climate in marine and terrestrial ecosystems. *Science* **334**, 652–655 (2011).
9. Ekau, W., Auel, H., Poertner, H.-O. & Gilbert, D. Impacts of hypoxia on the structure and processes in pelagic communities (zooplankton, macroinvertebrates and fish). *Biogeosciences* **7**, 1669–1699 (2010).
10. Stramma, L., Schmidtko, S., Levin, L. A. & Johnson, G. C. Ocean oxygen minima expansions and their biological impacts. *Deep-Sea Res. I* **57**, 587–595 (2010).
11. Clayton, T. D. & Byrne, R. H. Spectrophotometric seawater pH measurements: total hydrogen ion concentration scale calibration of m-cresol purple and at-sea results. *Deep-Sea Res. I* **40**, 2115–2129 (1993).
12. González-Dávila, M., Santana-Casiano, J. M., Rueda, M. J., Llinás, O. & González-Dávila, E. F. Seasonal and interannual variability of sea surface carbon dioxide species at the European Station for Time Series in the Ocean at the Canary Islands (ESTOC) between 1996 and 2000. *Global Biogeochem. Cycles* **17**, 1076 (2003).
13. Millero, F. J. The pH of estuarine seawater. *Limnol. Oceanogr.* **31**, 839–847 (1986).
14. Dickson, A. G., Sabine, C. L. & Christian, J. R. (Eds.) Guide to best practices for ocean CO_2 measurements. PICES Special Publication 3, IOCCP report No. 8 (2007).
15. Mintrop, L. *Versatile instruments for the determination of titration alkalinity. Manual for versions 3S and 3C* (2008).
16. Mehrbach, C., Culberson, C. H., Hawlay, J. E., & Pytkowicz, R. M. Measurement of the apparent dissociation constants of carbonic acid in seawater at atmospheric pressure. *Limnol. Oceanogr.* **18**, 897–907 (1973).
17. Dickson, A. G. & Millero, F. J. A comparison of the equilibrium constants for the dissociation of carbonic acid in seawater media. *Deep-Sea Res.* **34**, 1733–1743 (1987).
18. Santana-Casiano, J. M., González-Dávila, M. & Millero, F. J. Oxidation of nanomolar level of Fe(II) with oxygen in natural waters. *Environ. Sci. Technol.* **39**, 2073–2079 (2005).
19. González-Dávila, M., Santana-Casiano, J. M. & Millero, F. J. Oxidation of iron(II) nanomolar with H_2O_2 in seawater. *Geochim. Cosmochim. Acta* **69**, 83–93 (2005).
20. Konovalov, S. K. *et al.* Intercalibration of CoMSBlack-93a chemical data; unification methods for dissolved oxygen and hydrogen sulfide analyses and sampling strategies of CoMSBlack-94a cruise. *Rep. Inst. Mar. Sci. Edermil, Turkey.* (1994).
21. Konovalov, S. K. & Romanov, A. S. Spectrophotometric and iodometric methods for the detection of hydrogen sulfide in the Black Sea: comparison of the results of analysis. *Phys. Oceanogr.* **10**, 365–377 (1999).
22. Hernández-Brito, J. J., Cardona-Castellano, P., Siruela-Matos, V. & Pérez-Peña, J. A. High-speed computerized polarographic system for cathodic stripping voltammetry in seawater. *Electroanalysis* **6**, 1141 (1994).
23. Hernández-Brito, J. J., Gelado-Caballero, M. D., Pérez-Peña, J. & Herrera-Melián, J. A. Fast determination of Aluminum reactive to 1,2-Dihydroxyanthra-quinone-3-sulfonic Acid in Sea-Water. *Analyst* **119**, 1593–1597 (1994).
24. Marin, B., Nowack, E. C. M. & Melkonian, M. A plastid in the making: Evidence for a second primary endosymbiosis. *Protist* **156**, 425–432 (2005).
25. Marin, B. & Melkonian, M. Molecular Phylogeny and Classification of the Mamiellophyceae class. nov. (Chlorophyta) based on Sequence Comparisons of the Nuclear- and Plastid-encoded rRNA Operons. *Protist* **161**, 304–336 (2010).
26. Altschul, S. F., Gish, W., Miller, W., Myers, E. W. & Lipman, D. J. Basic Local Alignment Search Tool. *Journal of Molecular Biology* **215**, 403–410 (1990).
27. Gouy, M., Guindon, S. & Gascuel, O. SeaView version 4: a multiplatform graphical user interface for sequence alignment and phylogenetic tree building. *Molecular Biology and Evolution* **27**, 221-224 (2010).
28. Stamatakis, A. RAxML-VI-HPC: Maximum Likelihood-based Phylogenetic Analyses with Thousands of Taxa and Mixed Models. *Bioinformatics* **22**, 2688–2690 (2006).
29. Huelsenbeck, J. P. & Ronquist, F. MRBAYES: Bayesian inference of phylogeny. *Bioinformatics* **17**, 754–755 (2001).

Acknowledgments

This study has been supported by the Instituto Español de Oceanografía (I.E.O). The European project CARBOCHANGE-264879 has supported the analyses of carbon dioxide, reduced S species and Fe. We thank the Captain of the *R/V Ramón Margalef*, Luis Gago, and its crew for the help during this research.

Author contributions:

E.F-N. organised, designed and coordinated the study. M.G-D. and J.M.S-C carried out and interpreted the analyses of carbon dioxide, reduced S species and Fe. J.A. and M.F.M. conducted and interpreted the cytometric analyses. I.J.A-G and D.R.L. conducted and interpreted the total DNA extractaction, rDNA clone libraries and sequencing, and the alignment and phylogenetic analyses. S.H-L. and A.V.A. carried out and interpreted the acoustic measurements. M.J.B. carried out the geophysical studies. E.F-N., A.R-S., A.H-G., P.V-B., I.C-R. and V.M.B-B. conducted and interpreted the physical analyses. M.D.G-C. analysed and interpreted the soluble metals. F.E., J.M. and A.R. processed the satellite images. D.d.A. and J.F.D-Y. analysed and interpreted the oxygen data. All authors discussed the results and contributed to the final manuscript.

Additional information

Competing financial interests: The authors declare no competing financial interests.

How to cite this article: Fraile-Nuez, E. *et al.* The submarine volcano eruption at the island of El Hierro: physical-chemical perturbation and biological response. *Sci. Rep.* **2**, 486; DOI:10.1038/srep00486 (2012).